Comparison of CFD Prediction and Actual Condition for Wake Effect on an Onshore Wind Farm

Undarmaa Tumenbayar*, Jinhyuk Son*, Kyungnam Ko*‡

*Faculty of Wind Energy Engineering, Graduate School, Jeju National University, 102 Jejudaehakno, Jeju, 63243, Rep. of Korea

(undak69@jejunu.ac.kr, villyjin@jejunu.ac.kr, gnkor2@jejunu.ac.kr)

‡ Corresponding Author; Kyungnam Ko, Faculty of Wind Energy Engineering, Graduate School, Jeju National University, 102 Jejudaehakno, Jeju, 63243, Rep. of Korea, Tel: +82 64 754 4401, Fax: +82 64 702 2479, gnkor2@jejunu.ac.kr

Received: 25.05.2018 Accepted: 19.07.2018

Abstract- In order to clarify the wake effect behind wind turbines of a wind farm located on a complex terrain, Computational Fluid Dynamics (CFD) simulations were performed with the WindModeller software, which is a module for wind farm simulation developed by ANSYS. The wake is modelled using an actuator disc model approach which is based on the wind turbine thrust coefficient and wind speed. A WindModeller simulation was carried out for DBK wind farm located on Jeju Island, Korea. The nacelle wind speed data from 15 Hanjin 2MW turbines were collected through the Supervisory Control And Data Acquisition (SCADA) system. The wind data was measured from a 80m tall met mast near the wind farm, which was used as a reference. The WindModeller module simulated the wind speed and turbulence intensity within the terrain with a wind speed of 9.3 m/s and a wind direction of 314 degrees. The wakes from single and multiple turbines were predicted by the WindModeller simulation were compared with the actual wind data from the SCADA system. Then, the wake effect was analyzed with the distance between the wind turbines. As a result, the wake effect predicted by the WindModeller simulation was greater than the actual wake effect. The actual wind speed ratio decreased by 22% and 35% when the turbines were separated with the distances of 3.1 and 5.8 times rotor diameters, respectively. The wake effect behind multiple wind turbines is revealed in this paper.

Keywords wind energy; wind farm; CFD; wake effect; actuator disc.

1. Introduction

Humans have been making the environmental condition worse by using energy which results in the emission of greenhouse gases. The rapid growth in energy demand makes renewable energy more popular than other sources of energy. Out of all of the renewable energy resources, wind energy is gaining more popularity, because it is relatively economically viable [1]. The increasing demand for electricity is hastening the spread of wind turbines worldwide. Lots of investigations on wind resource assessment have been widely conducted worldwide [2-6]. Since wind farms have been generally situated on flat and gentle terrains, the chance of siting wind turbines on a complex terrain is very high for onshore wind farms [7-9].

The wind turbine layout is the most important factor for obtaining the maximum performance in a site. Energy production and the investment fund will fluctuate depending on the turbine layout. The wake behind wind turbines have great influence on the output of a wind farm [10]. Investigations on the turbine wake effect have been performed for the last two decades, since the wake causes a wind speed deficit and higher turbulence [11]. In other words, the wake effect within a wind farm is an unavoidable issue and the turbines affected by the wake produce electricity with about a 10-20% loss. In addition, a powerful velocity deficit comes from upwind turbines, which results in an increase in turbulence intensity [12-13]. CFD technique has been used for wind resource assessment, turbine blades design, etc. [14-16]. It is necessary to investigate the wake effect further using CFD technigue for achieving better wind turbine layouts.

This study aims to clarify the wake effect behind wind turbines in a real onshore wind farm through a CFD simulation. A CFD analysis was performed for the wind farm, and the wake effect predicted by the analysis was compared with the real wind data measured by nacelle anemometers. The wake effect behind the single and multiple turbines was discussed in terms of wind speed and turbulence intensity. In addition, the wind speed deficit and turbulence intensity were revealed in accordance with the distance between the turbines.

2. Site Description

Fig. 1a shows the location of DBK Wind Farm on Jeju Island, Korea. Jeju Island is situated off the southern coast of the Korean peninsula. The wind farm is located on the northeastern part of Jeju Island. Fig. 1b shows the layout of the DBK wind farm with a total of 15 Hanjin 2MW wind turbines. An 80m tall met mast is installed 220m north from wind turbine no. 15. There are three quarries and one landfill in the farm, which make the terrain complex.

(a) The location of DBK wind farm on Jeju Island

(b) DBK wind farm layout

Fig. 1 The location and layout of DBK wind farm

Table 1 shows site and measurement conditions. The 10 minute average wind condition is measured by an anemometer and a wind vane on an 80m tall met mast. The date and time of January 13th, 2017 at 4:20 am was applied for the CFD simulation, when the wind speed and direction on the met mast were 8.8 m/s and 314 degrees, respectively. The wind speed and direction data at the same time as the met mast were collected from the SCADA system of the farm for comparison with the CFD analysis result.

Table 1 Site and measurement conditions

Items	Category	Description
Site	Location	Latitude: 33°32'6.72"N
		Longitude: 126°42'53.85"E
	Capacity	30MW (2MW × 15)
	Altitude	49 m - 88 m
	Terrain complexity	RIX: 0.59
Wind turbine	Model	Hanjin HJW2000/87
	Rotor diameter/hub height	87m/80m
	Cut-in/rated/cut-out wind speed	3.5/12/25 m/s
Met mast	Location	Latitude: 33°32'28.22"N
		Longitude: 126°42'52.98"E
	Height	80m
	Anemometer	Ammonit Thies First Class
	Wind vane	Ammonit Thies First Class
	Wind data	10 min averaged
	Measurement date	4:20am 13th Jan 2017
SCADA	Model	Mitatech Gateway
	Measurement date	4:20am 13th Jan 2017

3. Modelling Condition

3.1 WindModeller software

The flow was simulated by using the Reynolds Averaged Navier Stokes (RANS) equations which was resolved by the WindModeller software with ANSYS CFX Ver. 17.0 [17]. WindModeller is a module developed for CFD analysis of wind farms by ANSYS. It uses the actuator disc model [18] for the wake which applies a finite-volume method of RANS for simulating the wake downwind from turbines within a wind farm.

The purpose of using of WindModeller is to conduct meshing and physical setups comparatively easily. The input information required for the meshing is terrain height and radius, grid resolutions, and the coordinates of the terrain. Physical models are mainly the turbulence model, atmospheric boundary layer inflow condition, forest canopy model, and wake model [19].

The actuator disc model is used in WindModeller for the analysis of wakes behind wind turbines. It calculates momentum loss when air flow passes wind turbine rotor blades for which it is necessary to give WindModeller the information of the wind turbine thrust coefficient with each wind speed and the wind speed at hub height. The turbine rotor faces to the local wind direction automatically [20-21,4]. Mesh adaption is carried out automatically on a wind turbine rotor for improving resolution.

The turbulence can be expressed by the k-ε or SST model in WindModeller [22-24]. The SST turbulence model is better than the k-ε model since it controls the flow separation better on a complex terrain.

3.2 Analysis condition

The conditions for the WindModeller simulation are presented in Table 2. The triangulation algorithm was implemented to create the terrain based on the numerical terrain map of the DBK wind farm [17]. The terrain with a radius of 5,000m and a height of 1,000m was created and the horizontal and vertical grid resolutions were 40m and 30m, respectively. To obtain a more accurate calculation result for the atmospheric boundary layer, the first vertical cell began at 7m above ground, followed by 30m above ground, and then increasing with an expansion factor of 1.15. There were 537,166 final elements for the wind farm in total.

Since the prevailing wind direction on DBK wind farm is from the northwest, 314 degrees was input for the simulation. The wind speed of 9.3m/s at 80m a.g.l. was used as a reference wind speed. The actuator disc model was used to predict the wake behind the wind turbines. The turbulence model of SST was used with the constant of 0.03 and a turbulence decay rate of 0.6.

Table 2 Parameters used in WindModeller simulation

Properties		Parameter
Meshing	Radius	5000 m
	Height	1000 m
	Horizontal resolution	40 m
	Vertical resolution	30 m
	First layer thickness	7 m
	Total mesh elements	537,166
Conditions	Wind direction	314 deg.
	Wind speed	9.3 m/s
	Wake model	Actuator disc model
	Turbulence model	SST

The inflow boundary conditions are given in the following equation [3]:

$$V_0 = \frac{V}{k}\ln\left(\frac{h_0}{h}\right) \quad (1)$$

where, V is velocity at the reference height, k is the Von Karman constant, then h_0 and h are the heights a.g.l.

Turbulence intensity is calculated over the terrain, which is given in the following equation [17]:

$$\mathrm{TI} = \frac{\sqrt{\frac{2}{3}k}}{V} \quad (2)$$

where, k is turbulence kinetic energy, V is local wind speed.

4. Result and Discussion

Fig. 2 shows the velocity distribution at the hub height of 80m with a wind direction of 314 degrees. The locations of the wind turbines are expressed by black rectangles with the turbine numbers, and the met mast is illustrated as well. The lower wind speeds are observed over the quarries and the landfill in the wind farm.

It is clear that the upwind turbines are not affected by the wake. The remaining turbines are affected by the wake from the upwind turbines. The wakes from turbines no. 2 and 15 give a direct impact on turbines no. 3 and 14. Turbines no. 11 and 12 are influenced by wakes from multiple upwind turbines. The wakes behind turbines no. 3 and 14 have a partial effect on the turbines no. 4 and 13, respectively. The wake effect behind the turbines goes downwind several kilometers. The velocity immediately behind turbines no. 3 and 14 decreases up to 40% compared with the upwind wind turbines.

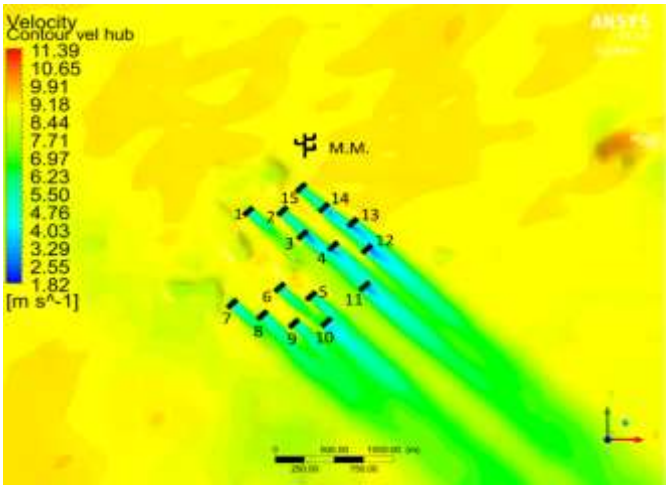

Fig. 2 Velocity distribution at hub height under a wind direction of 314 degrees

Fig. 3 shows the turbulence intensity distribution at a hub height of 80m a.g.l. with a wind direction of 314 degrees. A slightly higher turbulence intensity appears over the quarries and the landfill in the wind farm. Strong turbulence intensity can be found in the wake behind multiple wind turbines. The effect of the turbulence intensity persists for several kilometers downwind following the same trend as the velocity. Turbines no. 12 and 13 show a high turbulence intensity on one side of the rotor. Immediately behind the turbine rotor, the turbulence intensity increases, while velocity decreases as shown in Fig. 2. The turbulence intensity increases up to 0.42 immediately behind turbine no. 13. Also, the turbines experiencing the wake from multiple turbines show a very high turbulence intensity compared to other turbines.

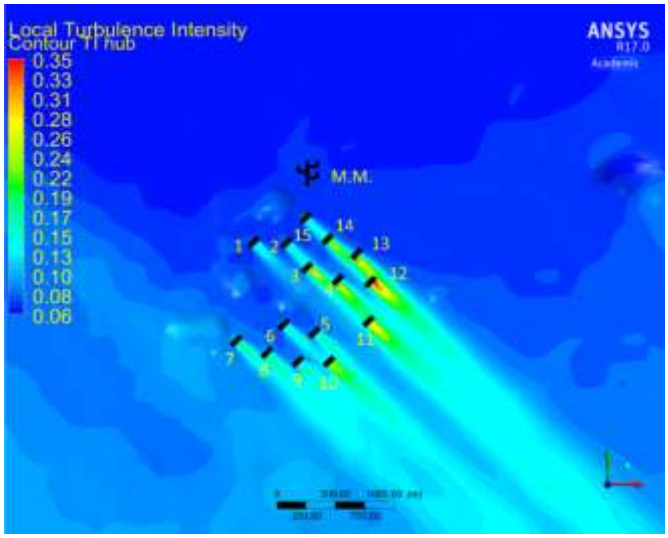

Fig. 3 Turbulence intensity distribution at hub height under a wind direction of 314 degrees

The predicted wind speed was extracted from a point immediately in front of the actuator disc in the WindModeller simulation, while the actual wind speed was collected from the SCADA system of the wind farm. Fig. 4 shows the comparison of actual and simulated wind speed ratios for both the simulated and the actual wind farm. The velocity ratio is defined in the following equation.

$$\text{Velocity ratio} = \frac{Nacelle\ wind\ speed}{Mast\ wind\ speed} \qquad (3)$$

Overall, the wake predicted by WindModeller is higher than the actual wake from the SCADA system. A 10% difference on average was found between the actual and the simulated wind speed ratios. There are a few reasons for the difference between the simulation and the measured data but it was mainly caused by the fact that the actuator disc converts the flow into turbulence immediately downwind [25]. The biggest difference between them appeared on turbine no. 8, which was about 17%, while turbine no. 9 had the smallest difference of 5.2%.

The turbines affected by the wake behind multiple turbines show the lower wind speed ratios compared with the other turbines. Since turbine no. 11 was affected by the wake from turbines no. 2 and 3, the simulated and the actual wind speed ratios were very low, which was less than 70%. On the other hand, turbine no. 14 also had significantly low ratios because it was directly influenced by the wake from turbine no. 15. Since the distance between the two turbines is comparatively short, only 3.1 times the rotor diameter, the speed ratios greatly decreased. However, the front row of turbines showed wind speed ratios of around 1.0 because they were not affected by the wake.

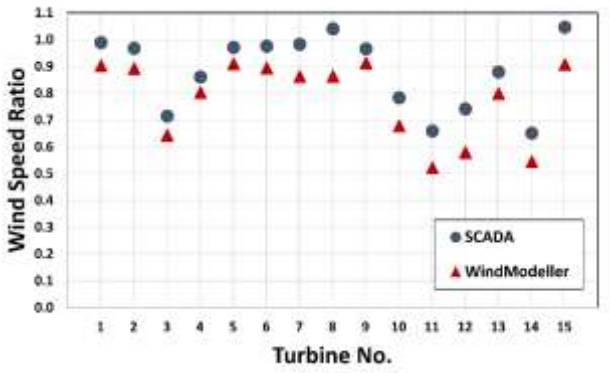

Fig. 4 Comparison of actual and simulated wind speed ratios of each turbine

Fig. 5 shows the distance between the upwind and the downwind turbines, which stems from an enlargement of Fig. 2. The figure shows that the wake effect changes depending on the distance between the turbines. In order to clarify the wake effect with the distance between the turbines, the representative wakes behind the single and multiple turbines were chosen on the wind farm. Single wakes were generated behind the turbines no. 6 and 15, which had an influence on turbines no. 10 and 14, respectively. The distances between each pair of the turbines are 5.8 D and 3.1 D, respectively. The wake was created by turbine no. 3 which was affected by the single wake from turbine no. 2, which had an influence on turbine no. 11. The distance between turbines no. 2 and 11 is 11.19 D, and each distance between the turbines is shown in the figure.

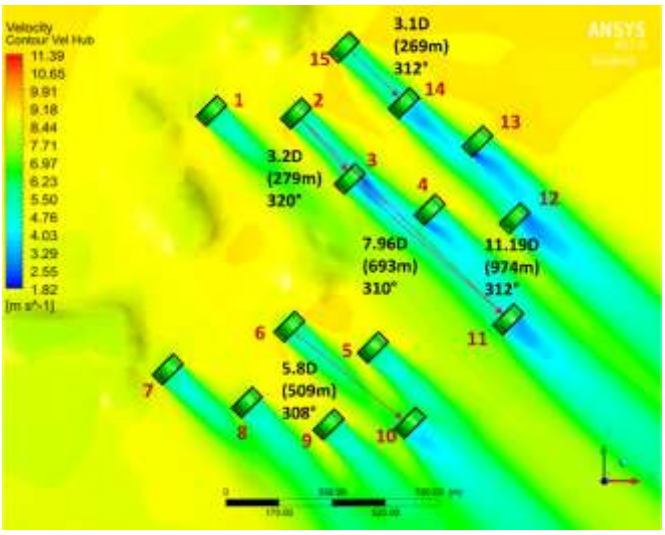

Fig. 5 Velocity distribution at hub height under a wind direction of 314 degrees and the distance between the turbines

A vertical cut was made along the line at 312 degrees shown in Fig. 5 for clarifying the wake effect from turbines no. 2, 3 and 11. Figs. 6 and 7 present the vertical velocity and turbulence intensity distributions. The velocity decreased behind turbine no. 2, and further decreased behind turbine no. 3. However, the velocity increased more and more by mixing with the surrounding air within the distance between turbines

no. 3 and 11. The velocity further decreased behind turbine no. 11, which then increased by mixing with the surrounding air.

The vertical turbulence intensity distribution was opposite to the vertical velocity distribution. The turbulence intensity immediately behind the turbine rotor was higher than the others. As the distance increased, the turbulence intensity decreased due to an increase of velocity with the further distance from the turbine rotor as shown in Fig. 6.

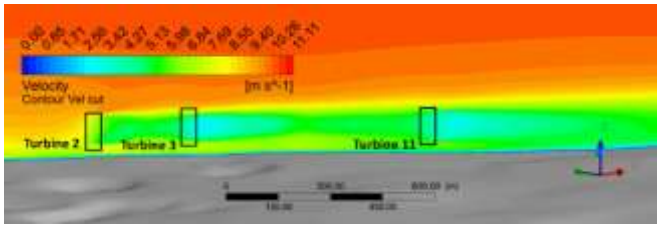

Fig. 6 Velocity distribution on a 312 degree vertical plane

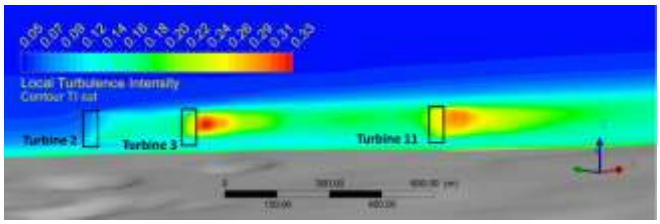

Fig. 7 Turbulence intensity distribution on a 312 degree vertical plane

Fig. 8 shows the comparison of the actual and the simulated wind speed ratios for a single wake with the distance between turbines. The actual wind speed ratio was about 10% higher than the simulated wind speed ratio. The actual and the simulated velocities increased as the distance between the turbines increased. For the distance of 3.1 D and 5.8 D, the actual wind speed ratios decreased by 35% and 22%, respectively.

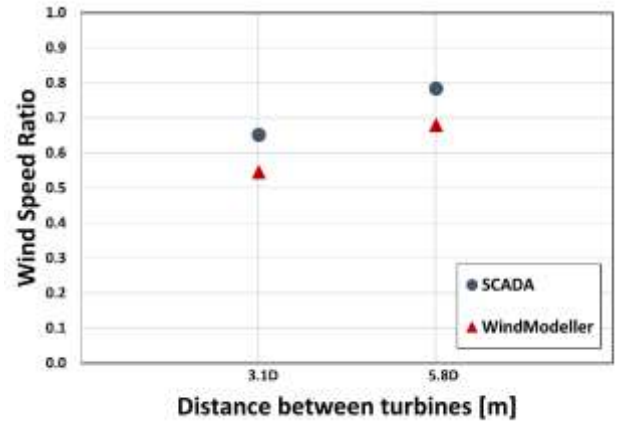

Fig. 8 Comparison of actual and simulated wind speed ratios for a single wake with the distance between turbines

Fig. 9 shows the comparison of the actual and the simulated wind speed ratios for the wake from multiple turbines. As shown in Fig. 5, since turbine no. 2 is located in the front row facing the wind, turbine no. 3 is affected by the single wake from turbine no. 2. Turbine no. 11 is also impacted by turbines no. 2 and 3. The simulated wind speed ratio was about 11% lower than the actual wind speed ratio. The wind speed ratio of turbine no. 11 was lower than the others. The actual wind speed ratios decreased by 28% and 34% for turbines no. 3 and 11, respectively.

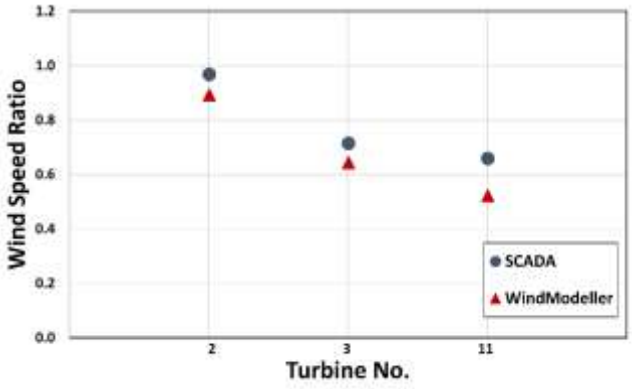

Fig. 9 Comparison of actual and simulated wind speed ratios for the wake from multiple turbines

5. Conclusion

The wake effect on DBK wind farm in operation on Jeju Island was investigated by comparing actual SCADA data from the wind farm with the result from a WindModeller simulation. The results are as follows:

1) It was found that the wind speed ratio predicted by WindModeller was about 10% lower than the real wind speed ratio from the SCADA data under the wind farm site conditions.
2) The actual and the simulated wind speed ratios decreased by 35% and 45%, respectively, for the distance of 3.1 D, while they reduced by 22% and 32%, respectively, for the distance of 5.8 D.
3) Turbine no. 11 showed a 34% loss for the actual wind speed ratio and a 48% loss for the simulated wind speed ratio because of the wake from upwind turbines no. 2 and 3.
4) From the WindModeller simulation, the trend of the turbulence intensity distribution was opposite to that of the velocity distribution on the wind farm.
5) It was possible to estimate the individual turbine's energy loss caused by the wake from the upwind turbines using CFD modelling.

Acknowledgements

This research was supported by the 2017 scientific promotion program funded by Jeju National University.

References

[1] A.Z. Dhunny, M.R. Lollchund, S.D.D.V. Rughooputh, Wind energy evaluation for a highly complex terrain using Computational Fluid Dynamics (CFD), Renewable Energy 101, pp.1-9, 2017.

[2] Izelu, C. Okechukwu, Agberegha, O. Larry, Oguntuberu, O. Bode, Wind Resource Assessment for Wind Energy Utilization in Port Harcourt, River State, Nigeria, Based on Weibull Probability Distribution Function, INTERNATIONAL JOURNAL of RENEWABLE ENERGY RESEARCH, Vol.3, No.1, 2013.

[3] R. K. Pachauri, Y. K. Chauhan, Assessment of Wind Energy Technology Potential in Indian Context, INTERNATIONAL JOURNAL of RENEWABLE ENERGY RESEARCH, Vol.2, No.4, 2012.

[4] M. A. Abdraman, A. M. Tahir, D. Lissouc, M. Y. Kazet, R. M. Mouangue, Wind Resource Assessment in the City of N'djamena in Chad, INTERNATIONAL JOURNAL of RENEWABLE ENERGY RESEARCH, Vol.6, No.3, 2016.

[5] R. J. de Andrade Vieira, M. A. Sanz-Bobi, S. Kato, Wind Turbine Condition Assessment based on Changes Observed in its Power Curve, International Conference on Renewable Energy Research and Applications, 2013.

[6] Abas Hossieni, Vahid Rasouli, Simin Rasouli, Wind Energy Potential Assessment In Order to Produce Electrical Energy for Case Study in Divandareh, Iran, 3rd International Conference on Renewable Energy Research and Applications, 2014.

[7] R. Spence, C. Montavon, I. Jones, C. Staples, C. Strachan, D. Malins, Wind modelling evaluation using operational wind farm site, EWEC Processing, 2010.

[8] C. Montavon, I. Jones, C. Staples, C. Strachan, I. Gutierrez, Practical issues in the use of CFD for modelling wind farms, EWEC Processing, 2009.

[9] C. Montavon, I. Jones, D. Malins, C. Strachan, R. Spence, Modelling of wind speed and turbulence intensity for a forested site in complex terrain, EWEC Processing, 2012.

[10] P. McKay, R. Carriveau, D. S-K Ting, T. Newson, Chapter 3 Turbine wake dynamics, Advances in Wind Power, 2012.

[11] V. L. Okulov, I. V. Naumov, R. F. Mikkelse, J. N. Sørensen, Wake effect on a uniform flow behind wind-turbine model, Journal of Physics: Conference Series 625, 2015.

[12] E. S. Politis, J. Prospathopoulos, D. Cabezon, K. S. Hansen, P. K. Chaviaropoulos, R. J. Barthelmie, Modelling wake effects in large wind farms in complex terrain: the problem, the methods, and the issues, Wind Energy 15, pp. 161-182, 2015.

[13] J. Bartl, F. Pierella, L. Sætran, Wake measurements behind an array of two model wind turbines, Energy Procedia 24, pp.305 – 312, 2012.

[14] Mikhail Ramos D., Daniel Sauceda C., CFD Study of a Vertical Axis Counter-Rotating Wind Turbine, 6th International Conference on Renewable Energy Reseach and Application, 2017.

[15] H. Salem, A. Diab, Z. Ghoneim, CFD Simulation And Analysis Of Performance Degradation Of Wind Turbine Blades In Dusty Envirnonments, International Conference on Renewable Energy Research and Applications, 2013.

[16] I. Colak, M. S. Ayaz, K. Boran, CFD Based Wind Assesment in West of Turkey, 4th International Conference on Renewable Energy Research and Applications, 2015.

[17] Ko Kyung-Nam, Huh Jong-Chul, Estimation of the wake caused by wind turbine and complex terrain by CFD wind farm modelling, Journal of the Korean Solar Energy Society 31, pp.19-26, 2011.

[18] R. Mikkelsen, Actuator Disc Methods Applied to Wind Turbines, 2003.

[19] WindModeller user manual, ANSYS Confidential, 2014.

[20] S. Roma Solanellas, C. Montavon, D. Madueno, A. Moragrega, S. Espana, Sensitivity of wake losses to wind turbine diameter for a offshore wind farm, EWEC Processing, 2014.

[21] C. Montavon, I. Jones, C. Sander, Accounting for stability effects in the simulation of large array losses, EWEC Processing, 2012.

[22] P. Argyle, S. Watson, C. Montavon, I. Jones, M. Smith, Turbulence intensity within large offshore wind farms, EWEC Processing, 2015.

[23] C. Montavon, G. Ryan, C. Allen, P. Housley, C. Staples and I. Jones, Comparison of meshing approaches and RANS turbulence models performance for flows over complex terrain, EWEC Processing, 2010.

[24] ANSYS CFX – Solver Theory Guide, pp.102-103, 2011.

[25] M. E. Harrison, W. M. J. Batten, L. E. Myers, A. S. Bahaj, A comparison between CFD simulation and experiments for predicting the far wake of horizontal axis tidal turbines, IET Renewable Power Generation, 2010.